3D Habitat Mapping Using High-Resolution Optical Satellite and Lidar Data

Amani, Meisam; Foroughnia, Fatemeh; Moghimi, Armin ; Mahdavi, Sahel

DOI
10.1109/Agro-Geoinformatics55649.2022.9859127

Publication date
2022

Document Version
Final published version

Published in
Proceedings of the 2022 10th International Conference on Agro-geoinformatics (Agro-Geoinformatics)

Citation (APA)
Amani, M., Foroughnia, F., Moghimi, A., & Mahdavi, S. (2022). 3D Habitat Mapping Using High-Resolution Optical Satellite and Lidar Data. In *Proceedings of the 2022 10th International Conference on Agro-geoinformatics (Agro-Geoinformatics)* (pp. 1-5). Article 9859127 IEEE. https://doi.org/10.1109/Agro-Geoinformatics55649.2022.9859127

3D Habitat Mapping Using High-Resolution Optical Satellite and Lidar Data

Meisam Amani
Wood Environment and Infrastructure Solutions
Ottawa, Ontario, Canada
meisam.amani@woodplc.com

Fatemeh Foroughnia
Department of Geoscience and Engineering
Delft University of Technology
Delft, The Netherlands
f.foroughnia@tudelft.nl

Armin Moghimi
Institut for Photogrammetriy and GeoInformation, Leibniz University,
Honnover, Germany
moghimi@ipi.uni-hannover.de

Sahel Mahdavi
Wood Environment and Infrastructure Solutions
Ottawa, Ontario, Canada
sahel.mahdavi@woodplc.com

2022 10th International Conference on Agro-geoinformatics (Agro-Geoinformatics) | 978-1-6654-7078-0/22/$31.00 ©2022 IEEE | DOI: 10.1109/AGRO-GEOINFORMATICS55649.2022.9859127

***Abstract*—Remote sensing datasets are great resources to map habitat types. In this study, 3D habitat maps were generated using high-resolution multispectral imagery and a LiDAR-derived digital surface model (DSM). Two study areas in the United Kingdom (UK) were selected to investigate the potential of the developed models in habitat classification. The overall classification accuracies for the two study areas were high (91% and 82%), indicating the satisfactory performance of the developed approach for habitat mapping in the study areas. Overall, it was observed that a synergy of high-resolution multi-spectral imagery and LiDAR data could provide reliable 3D information on habitat types.**

Keywords—habitat, 3D habitat mapping, Worldview-2, LiDAR

I. Introduction

Human activities and climatic change cause pressure on global biodiversity [1]. Effective strategies should be developed to mitigate serious habitat loss and further biodiversity extinction [2]. Accurate identification of land cover and land use types is prerequisite for habitat studies. Direct and indirect multi-temporal information on the extent of habitat types, regeneration landscapes, and land cover dynamics is required for various conservation planning activities. Progress toward habitat protection goals has been made by satellite imagery and monitoring techniques at

different spatial and temporal scales [3]. It has been well argued that remote sensing is a cost-effective tool to contribute to frequent natural habitat mapping over large areas [4, 5]. Various remote sensing datasets, ranging from multi-spectral and hyper-spectral imagery to Radar and LiDAR products can be employed in this regard. Remotely-sensed data help discriminate different vegetation types (forests, grasslands, and wetlands) and landscape structures [4, 6-8]. Machine learning methods have been widely employed to map habitat types for different areas. Kwong et al., [4] developed a multi-stage approach, which integrates remote sensing images, a GIS database and post-classification rules, to facilitate productive mapping of various habitat types in heterogeneous landscapes,. Adamo et al., [6] proposed a multi-disciplinary approach to grassland ecosystem classification, supported by expert ecologists as well as remote sensing experts. Using ecological coral habitat mapping and empirical modeling, Roelfsema et al. [5] documented the composition of shallow coastal reefs based on remote sensing data.

Although the above-mentioned studies have provided valuable information in the field of habitat mapping, using three-dimensional data and producing three-dimensional habitat maps has rarely been addressed. The main objective of the current research is to produce 3D habitat maps using a combination of high-resolution multispectral imagery and a LiDAR-derived digital surface model (DSM). An object-based Random Forest (RF) classifier was used to map habitat types of two case studies in the UK.

II. Method and Materials

A. Study area and data sets

Two study areas in northern England, including Colt Crag Reservoir, Northumberland, and Grassholme Reservoir, north Pennines AONB area, were selected to investigate the potential of the developed models for producing 3D habitat maps (See Fig. 1). These Reservoirs have high biodiversity of benthic habitats.

In this study, the Worldview-2 multi-spectral satellite images were employed to separate different habitat classes. The images have a spatial resolution of 2m and contain the spectral bands of visible range, near-infrared, and shortwave infrared, which are well-suited to discriminate different habitat types. Furthermore, LiDAR data were used to increase the classification accuracy and generate 3D maps. In this study, the LiDAR products, such as Digital Elevation Model (DEM) and Digital Surface Model (DSM), with a spatial resolution of 1m, provided by the UK Environment Agency (available through https://environment.data.gov.uk/DefraDataDownload/?Mode=survey) were utilized (see Fig. 1).

Moreover, several global positioning system (GPS) point samples were collected for each habitat types during field surveys. All the field samples were randomly split into two sets of training (50%) and testing (50%). The training set was used for training the machine learning classifier and the testing set was used for the statistically assessment of the accuracy of the results.

B. Methodology

Fig. 2 presents a flowchart of the proposed method to produce 3D habitat maps. More detail of each step of the proposed method is briefly elaborated in next paragraphs.

The geometric, radiometric, and orthorectification accuracies of Worldview-2 images were first investigated to assure they are suitable for the remote sensing model. Furthermore, exciting clouds were removed from images using a cloud-masking algorithm. Using a pan-sharpening method, the multispectral optical image was further sharpened to its pan image from 2 m to 0.5 m.

978-1-6654-7078-0/22/$31.00 ©2022 IEEE

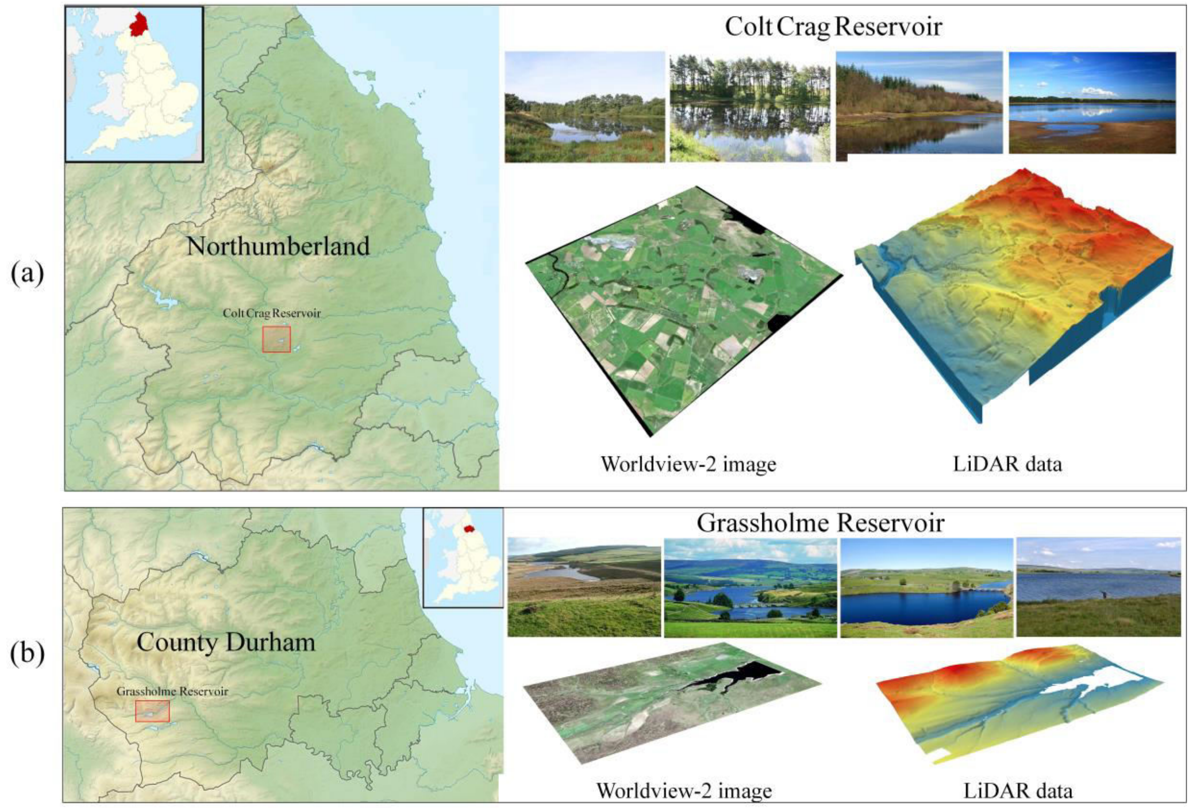

Fig. 1. The study areas and their remote sensing datasets used; (a) the location of Colt Crag Reservoi, and (b) Grassholme Reservoir in England and corresponding Worldview-2 images and Lidar datasets.

To ingest the multi-spectral images and DSM into the classification process, they were first mosaiced, co-registered, and layer-stacked. Also noteworthy is the fact that ArcGIS and several open-source software packages are employed for processing input data.

In cases where high spatial resolution images are available, object-based classification is often preferred to pixels-based classification [9]. Thus, object-based image analysis was led in this study to produce accurate habitat maps. The multiresolution segmentation algorithm was used to segment the multi-spectral images because it considers both the local and global characteristics of the imagery ad usually results in suitable segments [10, 11]. The *eCognition* software package was used to perform the segmentation, which includes hundreds of valuable toolboxes that can be applied to improve the classification accuracy compared to normally used software packages, like ArcGIS.

In order to improve the mapping accuracy, spectral and elevation features should be incorporated into the classification algorithm. Further, since this study employed object-based image analysis, multiple spatial and textural features were also included in the classification process to enhance accuracy.

In more detail, the Blue, Green, Red, and Near Infrared channels were used as main optical spectral bands in the classification process. Ratio of these spectral bands (e.g., $\frac{Blue}{Brightness}$, $\frac{Green}{Brightness}$, $\frac{Red}{Brightness}$, $\frac{Infrared}{Brightness}$), and some popular spectral indices derived from them like Normalized Difference Water Index= $\frac{\mathrm{Green-NIR}}{\mathrm{Green+NIR}}$, Normalized Difference Vegetation Index= $\frac{\mathrm{NIR-Red}}{\mathrm{NIR+Red}}$ were also stacked to main spectral bands to get better classification results. The main elevation (i.e., DEM and DSM) and elevation-derived features like Slope and Aspect were also employed as input beside of the spectral features. Moreover, texture features extracted form the Gray Level Co-occurrence Matrix (GLCM) and spatial features (e.g., Shape, Size, etc) are also used as inputs of proposed process.

Random Forest (RF) machine learning algorithms were used in this study to classify the input data. There are several decision trees in RF, and each of these includes nodes that are responsible for dividing the pixels into groups containing the most homogenous pixels. The process continues until each node represents a habitat class. Half of the field samples were used to train the RF algorithm.

The accuracy of the produced habitat maps is evaluated using two different methods. First, high-resolution imagery (e.g., those provided by ArcGIS and Google Earth) was analyzed to determine if the classes visually corresponded to natural landscapes. In the following step, we analyzed the confusion matrix derived from the test data (i.e., 50% of field samples) in order to measure the classification accuracy.

In the final step, the generated 2D-habitat map and LiDAR DSM were combined to produce the 3D maps of the study area. This step was implemented in ArcScene.

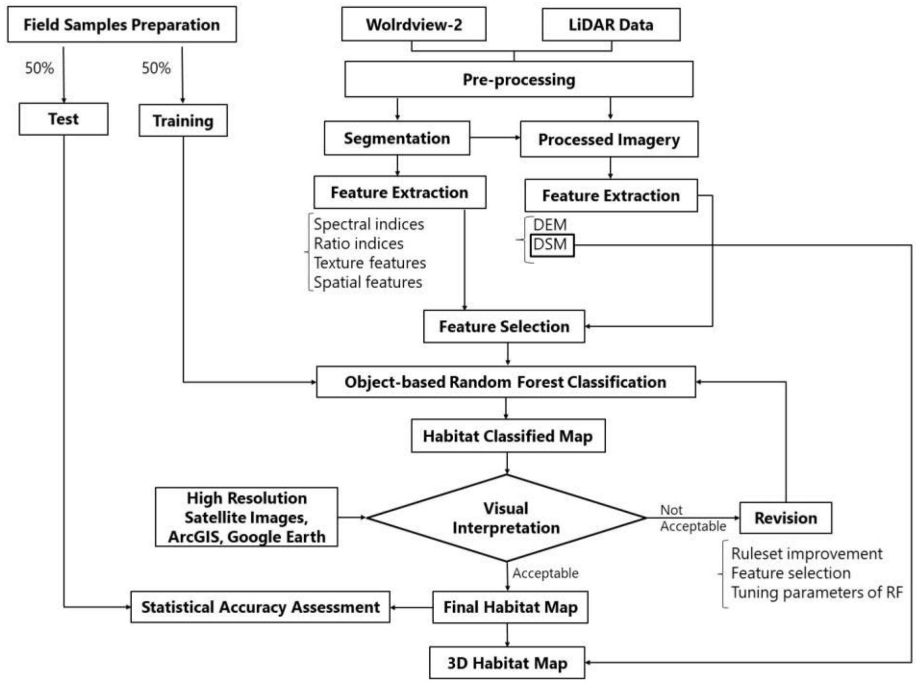

Fig. 2: The proposed model to produce 3D habitat maps using a combination of high resolution multi-spectral and LiDAR data.

III. RESULTS AND DISSCUSSION

Figure 3 shows the 2D and 3D classified habitat maps, achieved by the object-based RF classifier, which was ingested by a fusion of multi-spectral and LiDAR features. The most efficient features (except the spatial features) were ingested into the classification process. The 3D maps are obtained by combining the final classified habitat maps and LiDAR DSM data in ArcScene. A comparison analysis between resulted habitat maps and high-resolution multi-spectral images was done to evaluate accuracy of the result maps. It was concluded that the identified areas were in acceptable agreement with the reality. This confirmed the application of the proposed method in habitat mapping and discriminating habitat types.

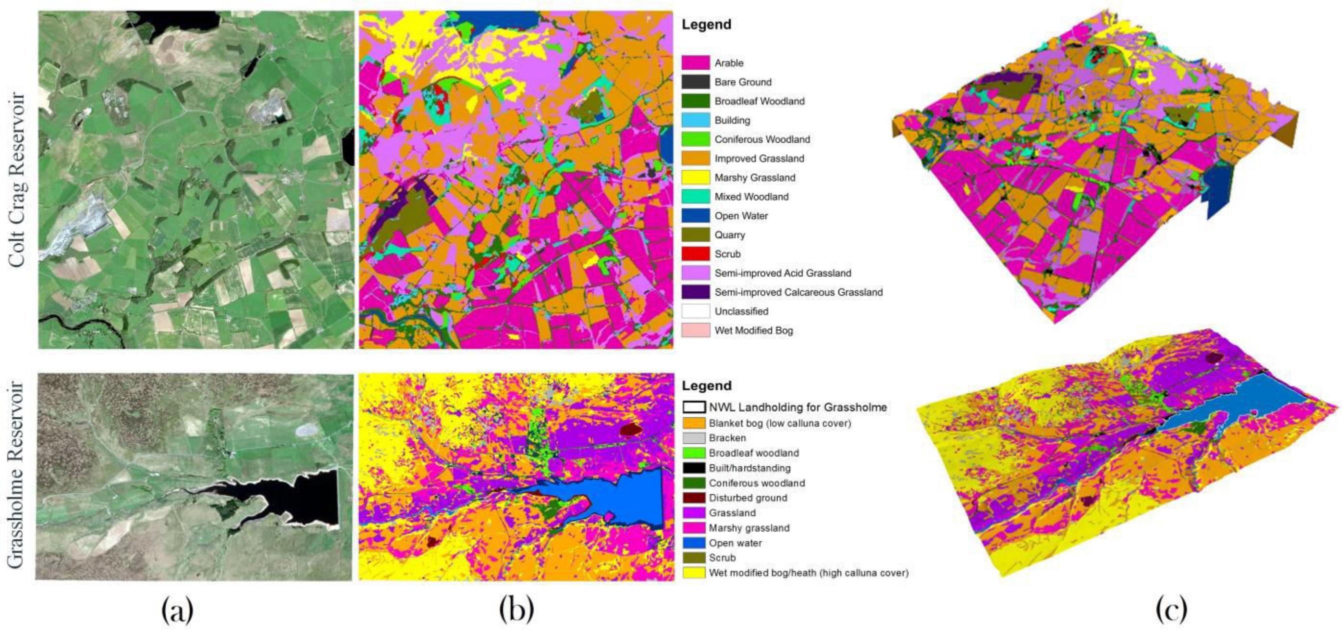

Fig. 3: (a) Worldview-2 multispectral satellite images; (b) 2D-habitat maps, and (c) 3D-habitat maps resulting from the proposed method for Grassholme and Colt Crag reservoirs.

The classification accuracies were also statistically assessed using the testing set (i.e., 50% of field samples) and analyzing the confusion matrices. The overall classification accuracies for Colt Crag Reservoir and Grassholme Reservoir areas were 91% and 82%, respectively, indicating the high performance of the used remote sensing approach for habitat mapping in the study areas. The producer and user accuracies for each habitat classes in the Colt Crag and Grassholme areas are also illustrated in Figure 4. The individual accuracies were considerably high for most of the habitat classes. According to the accuracy assessment results of the Colt Crag area, the Bare ground, Buildings, Coniferous woodland, Quarry, and Water classes were correctly classified in the final map without any misclassifications. This is because these classes have different spectral responses in satellite imagery. The accuracies of the Arable, Semi-improved acid grassland, Broadleaved woodland, and Wet Modified Bog were also considerably high. In contrast, some classes showed relatively low accuracy levels, e.g., Marsh/Marshy grassland class (25% producer accuracy). The reason could be the misclassification of marshlands as Semi-improved grassland. In contrast, the same class was identified with a higher accuracy (80%) in the Grassholme Reservoir area because there was no Semi-improved grassland class in this study area.

The main reason for the misclassification of some of the habitat classes was because they might have similar physical and spectral characteristics, and, thus, their spectral information could be allocated to a wrong class by a machine learning classifier. This can particularly rise to a challenge in differentiating habitat subclasses. LiDAR data, on the other hand, are essential for discriminating the habitat types with similar spectral responses but different elevations. For instance, LiDAR data are beneficial in discriminating the scrubs from woodlands. However, the relatively low accuracy in separating scrub from other woodlands was rooted in the relatively low resolution of the LiDAR data (i.e., 1 m).

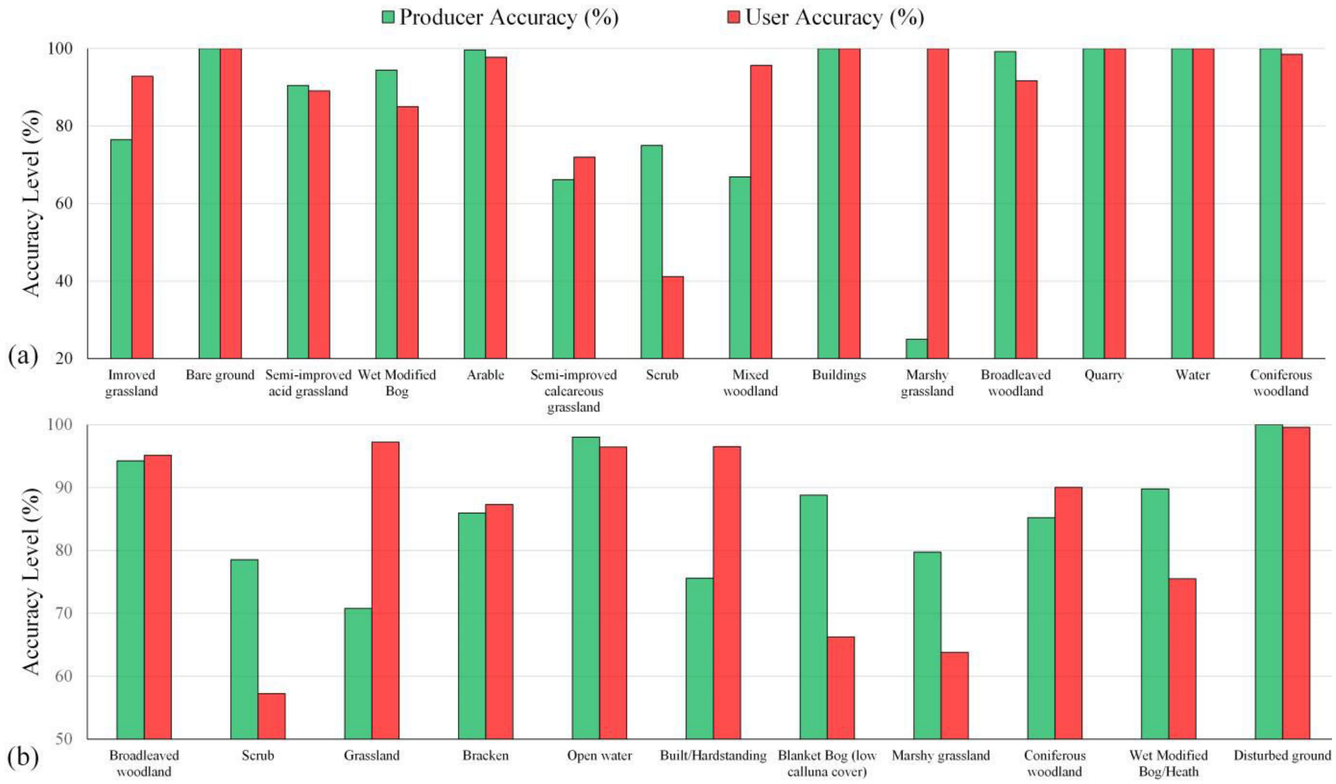

Figure 4. Producer and user accuracies for (a) the Colt Crag Reservoir, and (b) the Grassholme Reservoir.

IV. CONCLUSION

In this study, Worldview-2 imageries and LiDAR-derived DSM were used to map habitat types in two different case studies in UK using object-based Random Forest classification method. The results showed high classification accuracies for the habitat classes in the two study areas, indicating great potential of the proposed remote sensing approach in this paper. The results also indicated that a synergy of high-resolution multi-spectral imagery and LiDAR data could provide reliable 3D information on habitat types. LiDAR data are effective for discriminating the habitat types with similar spectral responses but different elevations.

REFERENCES

[1] O. E. Sala *et al.*, "Global biodiversity scenarios for the year 2100," *science,* vol. 287, no. 5459, pp. 1770-1774, 2000.

[2] T. M. Brooks *et al.*, "Global biodiversity conservation priorities," *science,* vol. 313, no. 5783, pp. 58-61, 2006.

[3] S. Luque, N. Pettorelli, P. Vihervaara, and M. Wegmann, "Improving biodiversity monitoring using satellite remote sensing to provide solutions towards the 2020 conservation targets," *Methods in Ecology and Evolution,* vol. 9, no. 8, pp. 1784-1786, 2018.

[4] I. H. Kwong, F. K. Wong, T. Fung, E. K. Liu, R. H. Lee, and T. P. Ng, "A Multi-Stage Approach Combining Very High-Resolution Satellite Image, GIS Database and Post-Classification

Modification Rules for Habitat Mapping in Hong Kong," *Remote Sensing,* vol. 14, no. 1, p. 67, 2021.

[5] C. Roelfsema *et al.*, "Coral reef habitat mapping: A combination of object-based image analysis and ecological modelling," *Remote Sensing of Environment,* vol. 208, pp. 27-41, 2018.

[6] M. Adamo *et al.*, "Knowledge-based classification of grassland ecosystem based on multi-temporal WorldView-2 data and FAO-LCCS taxonomy," *Remote Sensing,* vol. 12, no. 9, p. 1447, 2020.

[7] M. Amani *et al.*, "Google earth engine cloud computing platform for remote sensing big data applications: A comprehensive review," *IEEE Journal of Selected Topics in Applied Earth Observations and Remote Sensing,* vol. 13, pp. 5326-5350, 2020.

[8] H. Mohamed, K. Nadaoka, and T. Nakamura, "Towards benthic habitat 3D mapping using machine learning algorithms and structures from motion photogrammetry," *Remote Sensing,* vol. 12, no. 1, p. 127, 2020.

[9] A. Ghorbanian, M. Kakooei, M. Amani, S. Mahdavi, A. Mohammadzadeh, and M. Hasanlou, "Improved land cover map of Iran using Sentinel imagery within Google Earth Engine and a novel automatic workflow for land cover classification using migrated training samples," *ISPRS Journal of Photogrammetry and Remote Sensing,* vol. 167, pp. 276-288, 2020.

[10] M. Amani, S. Mahdavi, and O. Berard, "Supervised wetland classification using high spatial resolution optical, SAR, and LiDAR imagery," *Journal of Applied Remote Sensing,* vol. 14, no. 2, p. 024502, 2020.

[11] S. Mahdavi *et al.*, "Object-based classification of wetlands in Newfoundland and Labrador using multi-temporal PolSAR data," *Canadian Journal of Remote Sensing,* vol. 43, no. 5, pp. 432-450, 2017.